ELSEVIER

Cryogenics 40 (2000) 769–777

Cryogenics

www.elsevier.com/locate/cryogenics

Development of a thermal switch for faster cool-down by two-stage cryocooler ☆

Ho-Myung Chang *, Hyung-Jin Kim

Department of Mechanical Engineering, Hong Ik University, 72-1 Sangsu-Dong, Mapo-Ku, Seoul 121-791, South Korea

Received 27 November 2000; accepted 22 January 2001

Abstract

A gas-gap type thermal switch is developed to reduce the initial cool-down time of cryogen free magnets. The switch is a closed cylinder that contains several pairs of axial fins in staggered array and is filled with a gas. The switch connects the first and the second stages of a two-stage cryocooler (ON state) to take advantage of the large refrigeration capacity at the first stage. At cryogenic temperatures, however, the thermal isolation (OFF state) can be achieved without any external actuation, because the gas is frosted and the corresponding vapor pressure is significantly decreased. A detailed heat transfer analysis that takes into account the phase change, the gas convection in continuum or molecular state, and the axial conduction in the fins is presented. Based upon the analysis, a new configuration for the switch is proposed the transfers more heat during ON state and less heat during OFF state compared to the conventional structure. The two switches are fabricated and tested with a two-stage Gifford–McMahon cooler. The experiment shows that the newly developed gas-gap switch achieves a superior thermal performance. © 2001 Elsevier Science Ltd. All rights reserved.

Keywords: Heat transfer; Gifford–McMahon; Cryogen free magnet; Thermal switch

1. Introduction

Conduction–cooling method by cryogenic refrigerators can serve as an excellent option for relatively small superconducting systems [1–4]. Since no liquid cryogens are necessary, the systems are easier to operate and more compact in structure than the conventional liquid-cooling systems. In addition, the conduction-cooled systems are more efficient with respect to the energy consumption, mainly because the thermal loss associated with the storage and the transfer of cryogenic liquids is obviated. On the other hand, some difficulties have come out in recently developed liquid-free systems, one of which is a very long cool-down time required for initial operation.

For many practical systems cooled by a two-stage Gifford–McMahon cryocooler, the cool-down takes 10 h or even several days because of the limited refrigeration capacity at the second stage of the cryocooler. To achieve a faster cool-down rate, a simple device has been proposed, connecting thermally the first and the second stages during the beginning period in order to take advantage of the larger refrigeration capacity at the first stage as shown schematically in Fig. 1. After the cryogenic temperature is reached, however, the two stages should be thermally isolated in order to reduce the heat leak to the cold end in the final steady-state. The device has been called a thermal (or heat) switch, since the two required functions can be termed the thermally ON and OFF states, respectively.

Various types of cryogenic thermal switches have been introduced to date for different applications [4–11]. One of the candidates for the current application is the so-called gas-gap switch, since the ON/OFF operation is carried out only by the temperature without any mechanical or electrical actuation. The switch is a closed container, which has many pairs of thin extended surfaces or fins in staggered array, as shown in Fig. 2. The gap-space between the fins in the switch is filled with a gas to be condensed or frosted at cryogenic temperatures. When the switch is at temperatures higher than

☆ This paper was presented at the "Korea–Japan Joint Workshop on Applied Superconductivity and Cryogenics", Cheju-Do, Korea, October 2–4, 2000.

* Corresponding author. Tel.: +82-2-320-1675; fax: +82-2-322-7003.

E-mail address: hmchang@hongik.ac.kr (H.-M. Chang).

0011-2275/01/$ - see front matter © 2001 Elsevier Science Ltd. All rights reserved.
PII: S0011-2275(01)00034-0

Nomenclature

A	cross-sectional area
B	constants in solution of differential equations
Bi	Biot number
C	specific heat
i	specific enthalpy
k	thermal conductivity
Kn	Knudsen number
L	axial length of thermal switch
m	mass
P	pressure
q	heat transfer rate
R	gas constant
T	temperature
t	time
u	specific internal energy
V	volume
v	specific heat
W	sum of fin width
x	mass fraction of vapor
z	axial distance from cold end in thermal switch

Greek letters

α	accommodation coefficient of surface
γ	ratio of specific heats of gas
δ	gap clearance between fins, fin thickness
λ	mean free path of gas molecule

Subscripts

Cu	copper block at cold end
f	liquid phase
fin	fin
g	vapor phase
i	solid phase
LM	log mean
sat	saturated state
wall	wall of thermal switch
1	fin extended from the first stage end
2	fin extended from the second stage end
I	first stage of cryocooler
II	second stage of cryocooler

the saturation temperature of the gas, the gas serves as a fairly good heat transfer medium between the metal fins. At temperatures lower than the saturation temperature, liquid or solid begins to be deposited on the cold wall and the heat transfer between the fins diminishes due to low vapor pressure. In several previous studies, some qualitative design considerations have been presented for the purpose of constructing and testing selected prototypes of the switch. It can be stated, however, that any systematic and quantitative consideration for a comprehensive thermal design has not yet been taken.

This proposed study aims to investigate detailed heat transfer phenomena in the gas-gap thermal switch. The first part of this paper presents a straightforward heat transfer analysis for the staggered fins, to evaluate the effective heat transfer of the switch as a function of temperature. The second part describes two specific prototypes of the switch, which are fabricated and tested in a cool-down experiment by a miniature cryocooler. By examining the results from the analysis and the experiment, a few useful design issues are discussed for achieving faster cool-down by a two-stage cryocooler in practice.

2. Heat transfer analysis

The gas-gap thermal switch is a closed container that is filled with a gas. As the switch is cooled, the gas pressure decreases, since the volume occupied by the gas remains nearly constant. When the gas reaches the saturated state, it is either condensed into liquid or frosted into solid, depending on the size of its specific volume. Fig. 3 illustrates this cool-down process on a phase diagram of nitrogen. As the constant-volume process is indicated by a straight line on the diagram, it may be called a dew condition if the initial specific volume of gas is smaller than its value at triple point, and a frost condition otherwise.

It is assumed in this analysis that the gas in the switch behaves as an ideal gas. This assumption is valid in the rarefied (or molecular) state as well as in the continuum (or viscous) state, since the gas pressure is much lower than the critical pressure. When the gas temperature is higher than the saturation temperature, the gas pressure can be directly calculated as a function of temperature.

$$P = P(T) = \frac{mR}{V}T \quad \text{for } T > T_{\text{sat}}, \tag{1}$$

where m is the constant mass of the gas enclosed by the switch. If the gas temperature is distributed linearly in space, the temperature in Eq. (1) can be used as a log-mean.

$$T_{\text{LM}} = \frac{T_{\text{II}} - T_{\text{I}}}{\ln(T_{\text{II}}/T_{\text{I}})}, \tag{2}$$

where T_{I} and T_{II} are the two end temperatures.

When the liquid or solid is formed at lower temperatures, it may well be assumed that the gas has the saturation pressure because of the phase equilibrium on the surface of the liquid or solid.

$$P = P_{\text{sat}}(T) \quad \text{for } T \leqslant T_{\text{sat}}. \tag{3}$$

The mass fraction of the vapor (subscript 'g') in the saturated state is defined as

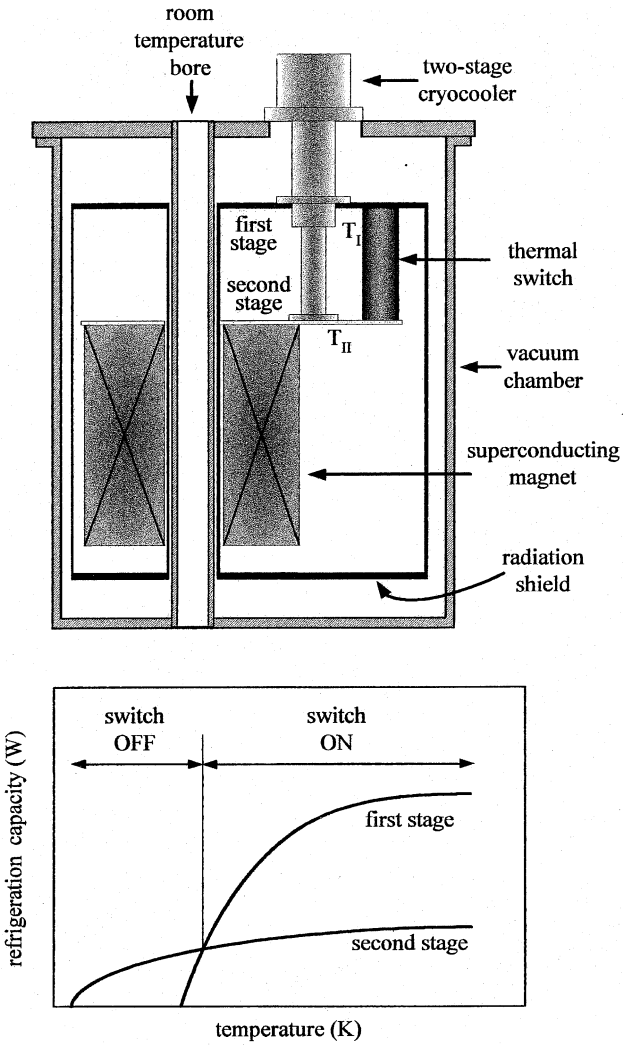

Fig. 1. Schematic representation of a superconducting magnet conduction-cooled by a two-stage cryocooler and refrigeration capacity at each stage as a function temperature.

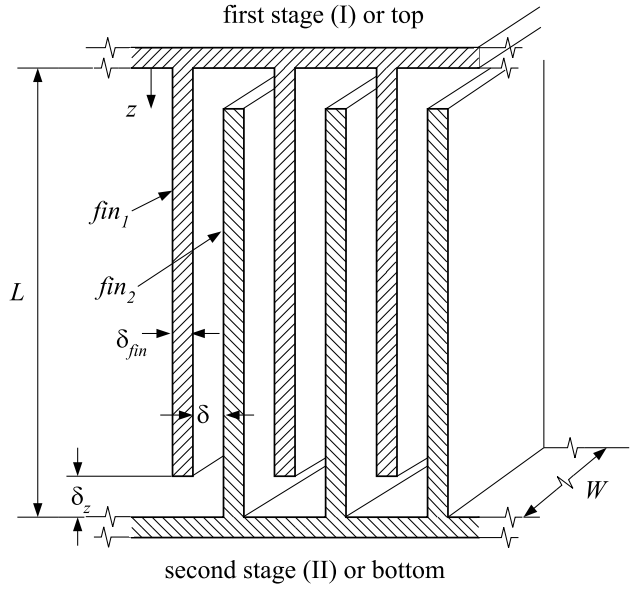

Fig. 2. Staggered array of fins in gas-gap thermal switch.

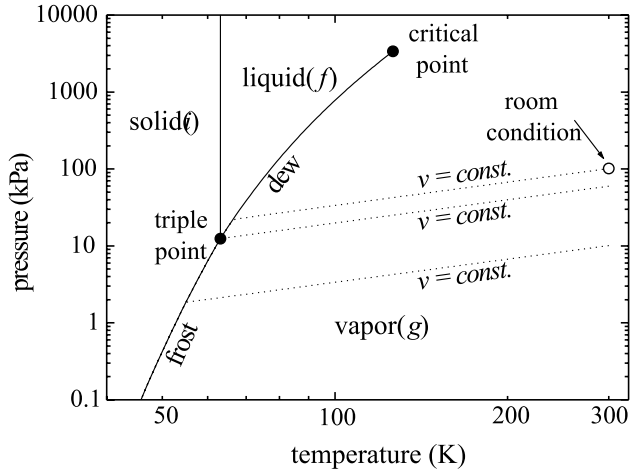

Fig. 3. Phase diagram of nitrogen with constant-volume lines.

$$x \equiv \frac{m_g}{m} = \frac{m_g}{m_f + m_g} \text{ or } x \equiv \frac{m_g}{m} = \frac{m_g}{m_i + m_g} \tag{4}$$

for the vapor–liquid (subscript 'f') or the vapor–solid (subscript 'i') equilibrium, respectively. It is also true that

$$v_g(T) = \frac{RT}{P_{sat}(T)} \gg v_f > v_i \text{ and } V \gg mv_f > mv_i. \tag{5}$$

The mass fraction of vapor is simply calculated as a function of temperature.

$$x = \frac{V - mv_i}{m(v_g - v_i)} \approx \frac{V}{mR}\frac{P_{sat}(T)}{T} \text{ or}$$
$$x = \frac{V - mv_f}{m(v_g - v_f)} \approx \frac{V}{mR}\frac{P_{sat}(T)}{T}. \tag{6}$$

It is now needed to estimate the convection heat transfer coefficient between the fins in the switch, before the temperature distributions can be determined along the fins. As the switch is cooled down to cryogenic temperatures, the vapor pressure decreases and the gas molecules get so far apart that the gas cannot be treated as a continuous medium. The dimensionless parameter for deciding the validity of the continuum is the Knudsen number, defined by

$$Kn \equiv \frac{\lambda}{\delta}, \tag{7}$$

where λ and δ are the mean free-path of the gas molecules and the clearance between the fins, respectively. The mean free-path is related to the viscosity of the gas, as given approximately by [13]. In general, the gas is treated as a continuum in the viscous state for $Kn < 0.01$ and as a rarefied gas in the molecular state or $Kn > 0.3$ [5,12,13]. The state for $0.01 < Kn < 0.3$ is called a mixed

or transition regime. In the continuum regime, the thermal conductivity of the gas is dependent mostly upon temperature. And the gas flow does not much affect the heat transfer, because the axial length of the fins is much greater than the gap clearance [8]. Therefore, the heat transfer coefficient between the fins can be simply expressed as

$$h(T) \approx \frac{k_g(T)}{\delta}. \tag{8}$$

In the rarefied gas regime, the heat transfer is more complicated, since the individual molecules carry the energy from one surface to another. A reasonable expression for the heat transfer between two parallel surfaces [5] is

$$h(T) \approx \alpha \frac{\gamma+1}{\gamma-1}\sqrt{\frac{R}{8\pi M}}\frac{P(T)}{\sqrt{T}}, \tag{9}$$

where γ and M are the ratio of specific heats and the molecular weight of the gas, respectively, and α is the so-called accomodation coefficient determined by the surface conditions. The pressure, P, in Eq. (9) is a function of temperature, as given by Eq. (1) or Eq. (3), depending on whether it is saturated or not. In most practical situations, of course, the rarefied gas will be in the frost condition so that the pressure can be taken as the saturation pressure.

Fig. 4 shows the heat transfer coefficient as a function of temperature, for the case in which the gap has a clearance of 1 mm and is charged with nitrogen gas at the atmospheric pressure and room temperature. The thermodynamic and thermophysical properties of nitrogen are obtained from a standard source [14]. The solid–vapor equilibrium data that is not provided by the source is approximated by way of the Clapeyron equation [15]. The accomadation coefficient, α, is taken as 0.8, which is valid for nitrogen gas on copper surfaces [5]. As indicated by the dotted curves, the heat transfer at the transition regime between the continuum and the rarefied gas is simply approximated by the two asymptotes. It should be noted that the heat transfer coefficient of rarefied gas is much lower by an order of magnitude.

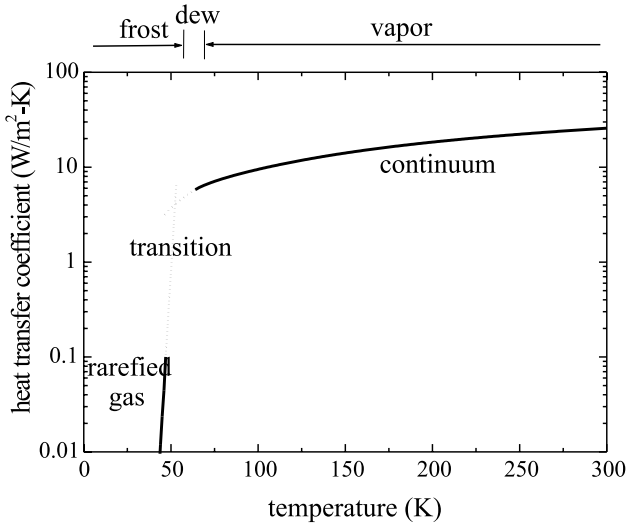

Fig. 4. Heat transfer coefficient as a function of temperature, when the gap clearance is 1 mm and the nitrogen gas is filled at the atmospheric pressure.

The next step of this analysis is to determine the temperature distribution of the fins, by use of the heat transfer coefficient described above. The temperature of the fin is considered to be one-dimensional along the axial (or z-) direction, since the Biot number is much smaller than unity.

$$Bi \equiv \frac{h\delta_{\text{fin}}}{k_{\text{fin}}} \ll 1. \tag{10}$$

In practice, Bi has an order of 10^{-4} or less, when taking the fin thickness, δ_{fin}, to have an order of 10^{-3} m, the thermal conductivity of copper, k_{fin}, to have an order of 10^2 W/m K, and the heat transfer coefficient, h, to have an order of 10 W/m^2 K or less from Fig. 4. The heat conduction equation can be written for a pair of fins as

$$\frac{d^2T_1(z)}{dz^2} = -\frac{2Bi}{\delta_{\text{fin}}^2}[T_2(z) - T_1(z)], \tag{11}$$

$$\frac{d^2T_2(z)}{dz^2} = \frac{2Bi}{\delta_{\text{fin}}^2}[T_2(z) - T_1(z)], \tag{12}$$

where $T_1(z)$ and $T_2(z)$ are the temperatures of the fins extended from the bottom and the top plates, respectively, as shown in Fig. 2. The right-hand sides of Eqs. (11) and (12) are multiplied by 2 because the exchange of heat takes place on both surfaces of the fin by symmetry.

Boundary conditions for the equations are given by the two end temperatures and the convection heat transfer at tips of the fins.

$$\begin{aligned} &T_1(0) = T_{\text{I}}, \quad T_2(L) = T_{\text{II}}, \\ &\frac{dT_2(\delta_z)}{dz} = \frac{Bi}{\delta_{\text{fin}}}[T_2(\delta_z) - T_{\text{I}}], \\ &\frac{dT_1(L-\delta_z)}{dz} = \frac{Bi}{\delta_{\text{fin}}}[T_{\text{II}} - T_1(L-\delta_z)]. \end{aligned} \tag{13}$$

The axial gap at the tips, δ_z, is usually much smaller than the total axial length, L, so it will be set at zero in the following analysis. In general, the Biot number is a function of temperature. As will be shown below, however, the axial temperature difference between the two ends is not large in a good switch. Thus, Bi is assumed to be a constant by taking the average. The solution of Eqs. (11) and (12) with the boundary conditions, Eq. (13), can be written in dimensionless forms as

$$\frac{T_1(z)-T_I}{T_{II}-T_I} = B_1 + B_2\frac{z}{L} + B_3\cosh\left(2\sqrt{Bi}\frac{z}{\delta_{fin}}\right) + B_4\sinh\left(2\sqrt{Bi}\frac{z}{\delta_{fin}}\right), \quad (14)$$

$$\frac{T_2(z)-T_I}{T_{II}-T_I} = B_1 + B_2\frac{z}{L} - B_3\cosh\left(2\sqrt{Bi}\frac{z}{\delta_{fin}}\right) - B_4\sinh\left(2\sqrt{Bi}\frac{z}{\delta_{fin}}\right). \quad (15)$$

The four constants in the solution, B's, are dimensionless and should be determined by a set of equations

$$\begin{bmatrix} 1 & 0 & 1 & 0 \\ 1 & 1 & -Ch & -Sh \\ 1 & -\frac{1}{Bi}\frac{\delta_{fin}}{L} & -1 & \frac{2}{\sqrt{Bi}} \\ 1 & 1+\frac{1}{Bi}\frac{\delta_{fin}}{L} & \frac{2}{\sqrt{Bi}}Sh+Ch & \frac{2}{\sqrt{Bi}}Ch+Sh \end{bmatrix} \begin{Bmatrix} B_1 \\ B_2 \\ B_3 \\ B_4 \end{Bmatrix} = \begin{Bmatrix} 0 \\ 1 \\ 0 \\ 1 \end{Bmatrix}, \quad (16)$$

where

$$Ch = \cosh\left(2\sqrt{Bi}\frac{L}{\delta_{fin}}\right) \text{ and } Sh = \sinh\left(2\sqrt{Bi}\frac{L}{\delta_{fin}}\right). \quad (17)$$

The exactness of this solution can be simply verified by substituting the temperature distributions into Eqs. (11)–(13). It is noted that the dimensionless temperatures are functions of z/L, being determined by only two parameters, Bi and L/δ_{fin}.

Fig. 5 illustrates typical axial temperature distributions of a pair of fins for various values of Bi, when $L/\delta_{fin} = 100$. As mentioned above, Bi has an order of 10^{-4} or less in the present problem. The temperature difference between the two fins increases as Bi or the heat transfer coefficient decreases. From the symmetry of Eqs. (11) and (12), the two curves are always convex in the opposite direction. Hence, the temperature difference should be smallest at an intermediate axial location of the switch.

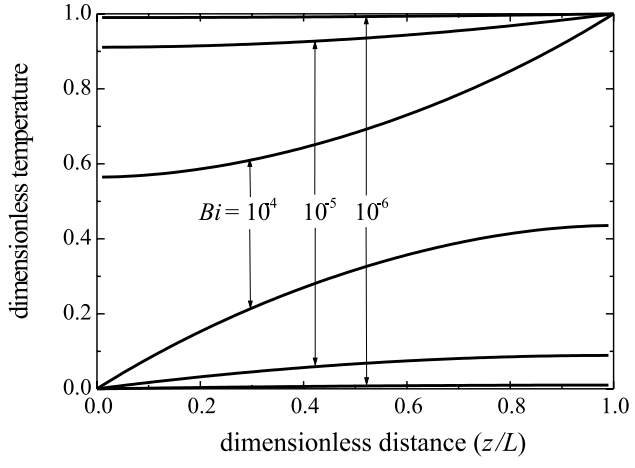

Fig. 5. Axial temperature distribution of fins for various Bi's, when $L/\delta_{fin} = 100$.

The final step of the present analysis is to estimate the overall heat transfer rate though the gas-gap thermal switch. Since heat may be transferred through the interior media (fins and gas) and the exterior wall, the overall heat transfer is the sum of the two

$$q = q_{wall} + q_{fin}. \quad (18)$$

The wall conduction is calculated simply from the integration of thermal conductivity.

$$q_{wall} = \frac{A_{wall}}{L}\int_{T_I}^{T_{II}} k_{wall}\,dT. \quad (19)$$

This heat should be minimized, of course, because it represents the refrigeration load in the final steady-state. The second term of Eq. (18) can be obtained from the axial temperature distribution of the fins and rearranged into a neat form by use of Eq. (16).

$$q_{fin} = \delta_{fin}W\left\{k_{fin}\frac{dT_1(0)}{dz} + h[T_2(\delta_z) - T_I]\right\} = 2k_{fin}W(T_{II}-T_I)\frac{\delta_{fin}}{L}B_2, \quad (20)$$

where W is the total width of the fin at one plate, as indicated in Fig. 2. The constant B_2 is so complicated function of Bi or h as shown in Eq. (16). If $(T_{II} - T_I)$ is significant, the thermal conductivity can be evaluated at the log mean defined by Eq. (2). The heat transfer rate expressed in Eq. (20) represents the significant result, as it predicts the thermal performance of the gas-gap switch. A few quantitative examples of the expression are presented in the following section.

3. Design and fabrication

Two different configurations of the gas-gap thermal switch are designed and fabricated in our laboratory. The first one (called Switch A) has basically the same structure as previous reported switches [4,6–8,10,11]. The appearance of Switch A is a hollow cylinder shown in Fig. 6. One major advantage of the hollow shape is that it can be placed to surround the cold finger of the cryocooler for a compact integration [4,8]. Four pairs of concentric-tube fins are attached to the top and the bottom plates to form a staggered array. The outer and inner diameters of Switch A are 60 and 30 mm, respectively, and the height is 100 mm, which is also the distance between the first and second stages of our miniature GM cryocooler to be used in the experiment.

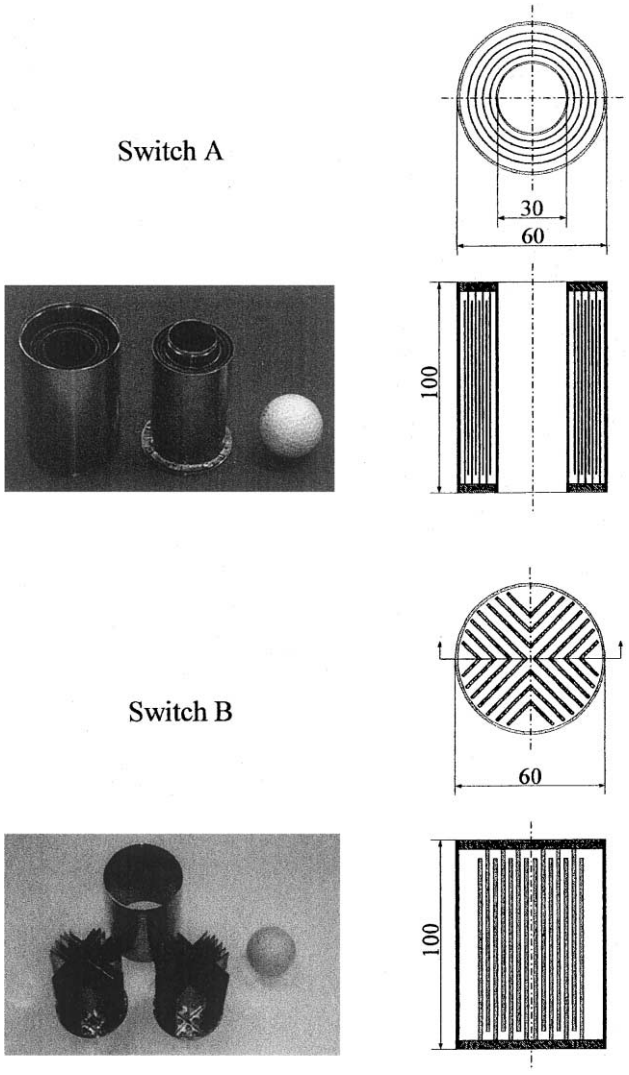

Fig. 6. Two different configurations of gas-gap thermal switch (unit: mm).

A different structure (called Switch B) which is a simple cylinder is proposed in this study. For a full use of the interior space near the axial center in Switch B, 14 pairs of plate fins bent in right angles are arranged in a staggered array, as shown in Fig. 6. To compare the thermal performance, the two switches are designed to have the same outer diameter and height. Switch B has the fin area of about 3.2 times that of Switch A, but has only two-thirds the cross-sectional area of the wall. The interior fins are made of copper plates whose thickness is 1 mm and all the exterior walls are made of the stainless steel.

The gas to fill the switches should be selected based on the temperature at which the thermal ON/OFF operation is switched. Since the switching temperature is in the range between 50 and 70 K for most two-stage coolers, the nitrogen is a good choice as shown in Fig. 3. When the two switches are charged with pure nitrogen at room temperature and atmospheric pressure, the overall heat transfer divided by the temperature difference, $q/(T_{II} - T_I)$, is calculated as described in the previous section and plotted as a function of cold end temperature in Fig. 7. In general, both switches function satisfactorily, as the heat transfer drops sharply at around 50–60 K. It is obvious, however, that Switch B will be superior to Switch A, because it carries more heat during ON state and less heat during OFF state.

The charging pressure or the mass of gas does affect the switching temperature. As the charging pressure increases, the saturation temperature also increases. In practice, however, its effect on the saturation temperature is not substantial at moderate pressures, since the slope of the vapor pressure curve is much greater than that of the constant-volume lines as demonstrated in Fig. 3. It is thus decided in the present design that the gas is charged at the atmospheric pressure. Furthermore, it may be a smart choice to use "air" instead of pure nitrogen, considering its much greater convenience during the assembly. The oxygen in air may result in a slightly higher switching temperature.

The copper fins are fixed on the top or the bottom plate by miniature bolts. Each sheet of the fin has an extra length to be bent as flange for the bolt joints. The tubular wall is welded with the top and the bottom plates to form a tight enclosure.

4. Experiment

The two gas-gap thermal switches described in the previous section are tested in our laboratory. Fig. 8 shows schematically a simple experimental apparatus constructed. A copper block of 9 kg mass is directly attached as thermal load to the second stage of a small two-stage GM cryocooler (Cryogenic Technology Model M22). The refrigeration capacity of the GM

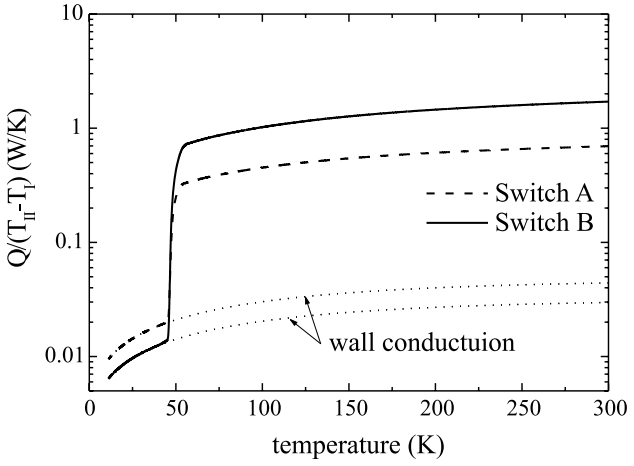

Fig. 7. Overall heat transfer rate as a function of temperature for the two switches.

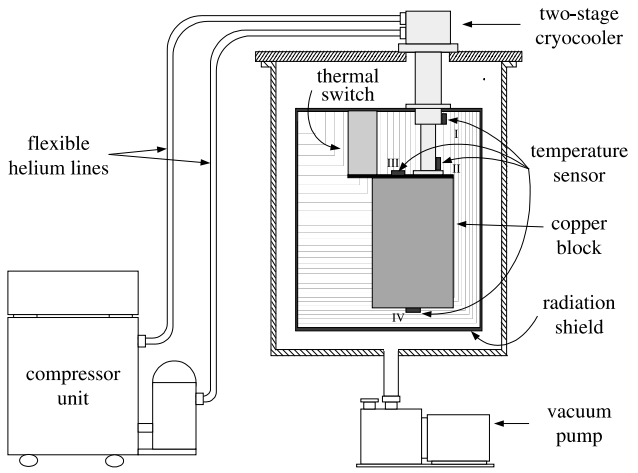

Fig. 8. Experimental apparatus and locations of temperature sensors.

cooler is as small as 1 W at 20 K for the second stage and 7 W at 77 K for the first stage. The thermal switch is located between the first and the second stages. As indicated in Fig. 8, temperature is measured every minute at four different locations; the first stage(I), the second stage(II), the top(III) and the bottom(IV) of the cold block. The temperature sensors are the silicon diodes (Lakeshore Model DT-470-SD-13). The radiation shield is conduction-cooled by the first stage of the cooler and multi-layer insulation is wrapped on the shield and around the cold parts. The cool-down experiment is repeated first without and then with the thermal switches employed.

5. Results and discussion

Fig. 9 shows the cool-down curves for three different cases: without the switch, with Switch A and with Switch B. For simplicity, only the temperatures at the first and second stages of the cooler are plotted in the graph. The temperature at the bottom of the copper block is observed to be higher by about 2–3 K than at the second stage, mainly because of thermal radiation to the surface of the block.

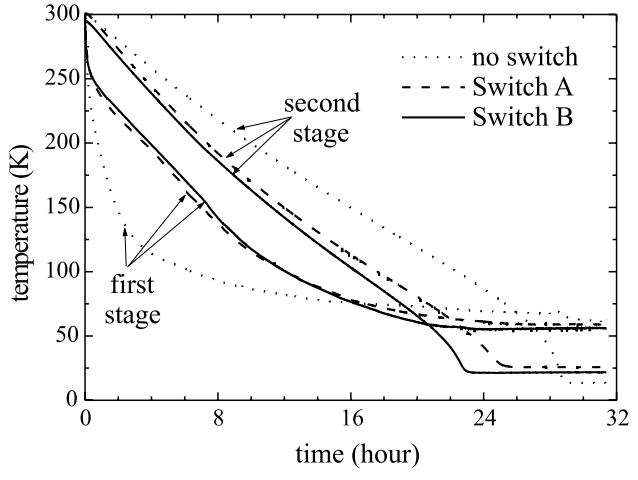

Fig. 9. Measured cool-down curves with and without a thermal switch.

In the case of no thermal switch, the second stage is cooled very slowly, while the first stage is cooled quickly at the initial stage because of its small load. It is noted that the two stages have the same temperature at around 70 K. The cool-down of the block is relatively faster at temperatures below 50 K because the specific heat of the copper gets smaller. It has taken approximately 23 h to cool down to 100 K, and 29 h to reach a steady state at 13 K.

By employing Switch A, the temperature difference between the two stages is significantly reduced at temperatures above 70 K, which means that the first stage has contributed to the cooling at the second stage. As a result, the cool-down time to 100 K is shortened by almost 5 h. At temperatures below 50 K, however, the cool-down is relatively slow so that the final cool-down time is shortened by only 4 h. The final steady-state temperature at the cold end is increased to 25 K. The reason is that the thermal switch in OFF state has added the heat leak to the cold end by its own wall conduction.

The cool-down characteristics with Switch B are basically the same as those with Switch A. As predicted from the analysis, the heat transfer is augmented at higher temperatures so that the temperature difference between the two stages can be slightly further reduced. The cool-down time to 100 K is about 16.5 h, which is shorter by 1.5 h than that with Switch A. It is also noted in this case that the cool-down speed can be maintained at temperatures lower than 50 K and that the final temperature reached is lower than that with Switch A. These improvements have been expected from the reduced wall conduction. The overall cool-down time is less than 23 h and the steady-state temperature is approximately 22 K.

Another interesting aspect of the improvement is associated with the location of the liquid in the switch. As shown in Fig. 3, the dew temperature of pure nitrogen is around 66 K. The cool-down curve for Switch A indicates that this temperature is reached by the second stage so that the gas may have been liquefied at the bottom of the switch. In the case of Switch B, the first stage is cooled to this dew point sooner, so that the gas may have been condensed at the top and have flowed down along the fins. If this is true, the fin-to-fin heat transfer would have been augmented for the short period of time.

The 21% reduction in the cool-down time may not be regarded as sufficient. The reduction is limited primarily due to the characteristics of the GM cryocooler, rather than the switch itself. The cooler employed in the pre-

sent experiment does not have enough refrigeration capacity at the first stage. To verify this quantitatively, the refrigeration capacity can be calculated from the cool-down data. In the case of no thermal switch, the refrigeration capacity can be estimated by the rate of energy decrease in the copper block.

$$q = -m_{\mathrm{Cu}} C_{\mathrm{Cu}} \frac{\mathrm{d}T_{\mathrm{II}}}{\mathrm{d}t}, \tag{21}$$

where the temperature-dependent specific heat and the slope of the curve in Fig. 9 are included. When a thermal switch is placed, the refrigeration capacity is the rate of energy decrease in both the copper block and the switch. While the air remains in the vapor phase, the capacity is simply

$$q = -m_{\mathrm{Cu}} C_{\mathrm{Cu}} \frac{\mathrm{d}T_{\mathrm{II}}}{\mathrm{d}t} - (m_{\mathrm{wall}} C_{\mathrm{wall}} + m_{\mathrm{fin}} C_{\mathrm{fin}} + mC_v) \frac{\mathrm{d}T_{\mathrm{LM}}}{\mathrm{d}t}. \tag{22}$$

The third term in the parenthesis of Eq. (22) is the heat capacity of the gas, which is of course negligibly small. If the gas is saturated, however, the cooling load caused by the phase change should be added for the saturated state. Therefore,

$$q = -m_{\mathrm{Cu}} C_{\mathrm{Cu}} \frac{\mathrm{d}T_{\mathrm{II}}}{\mathrm{d}t} - \left(m_{\mathrm{wall}} C_{\mathrm{wall}} + m_{\mathrm{fin}} C_{\mathrm{fin}} + m_{\mathrm{f}} C_{\mathrm{f}} + VT \frac{\mathrm{d}^2 P_{\mathrm{sat}}}{\mathrm{d}T^2} \right) \frac{\mathrm{d}T_{\mathrm{LM}}}{\mathrm{d}t} \tag{23}$$

for the dew condition and

$$q = -m_{\mathrm{Cu}} C_{\mathrm{Cu}} \frac{\mathrm{d}T_{\mathrm{II}}}{\mathrm{d}t} - \left(m_{\mathrm{wall}} C_{\mathrm{wall}} + m_{\mathrm{fin}} C_{\mathrm{fin}} + m_{\mathrm{i}} C_{\mathrm{i}} + VT \frac{\mathrm{d}^2 P_{\mathrm{sat}}}{\mathrm{d}T^2} \right) \frac{\mathrm{d}T_{\mathrm{LM}}}{\mathrm{d}t} \tag{24}$$

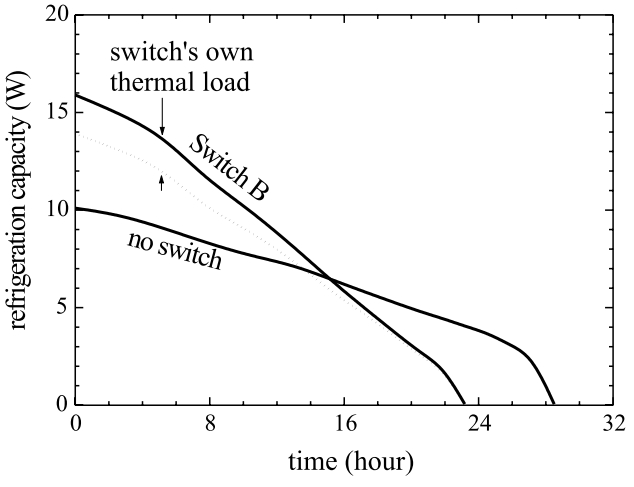

Fig. 10. Estimated refrigeration capacity at the first and second stages during cool-down.

for the frost condition. The third and fourth terms in the parenthesis of Eqs. (23) and (24) represent the derivative of the internal energy with respect to temperature in the saturated state, as derived in Appendix A. The refrigeration capacity is plotted in Fig. 10 as a function of time during the cool-down, for the cases of no switch and Switch B. By employing the switch, the overall refrigeration capacity has been increased by 60% for the cool-down period. In fact, only 40% of the refrigeration is effective in cooling the cold block, since the remaining portion is spent by the switch's own thermal load. The cool-down could be accelerated considerably with the same thermal switch by employing any cryocooler that has a greater capacity at the first stage.

6. Conclusions

A heat transfer analysis for predicting the thermal performance of the gas-gap switches is presented. The analysis includes the phase change of the vapor to the liquid or solid, the gas convection in the continuum or molecular state, and the axial heat conduction through the internal fins or the external walls. Based on the analysis results, a new improved switch configuration is proposed. A new switch structure is designed, fabricated, tested by an experiment, and compared with the conventional switch having the same outer size. The analytical prediction is experimentally verified, and both the cool-down time and the heat leak in the steady state are reduced. It is concluded that the presented analysis can be a useful design tool for achieving better thermal performance of the gas-gap switch.

Acknowledgements

Authors wish to thank Dr. B.H. Kang at Korea Institute of Science and Technology for his kind support of components of the experimental apparatus.

Appendix A

This appendix presents the derivation of a thermodynamic expression for the change of the internal energy in a constant-volume process with a phase change. While the following relations hold for a vapor(g)–solid(i) equilibrium, the same relations are also applicable to the vapor(g)–liquid(f) equilibrium if the subscripts i are replaced by f.

When a pure substance is in the saturated state, the internal energy per unit mass can be expressed in terms of the mass fraction of the vapor, defined by Eq. (4).

$$u = u_{\mathrm{i}} + x(u_{\mathrm{g}} - u_{\mathrm{i}}). \tag{A.1}$$

From the definition of the enthalpy and Eq. (5), the second term of Eq. (A.1) can be written as

$$x(u_g - u_i) = x\left[(i_g - i_i) - P_{sat}(v_g - v_i)\right] \approx x\left[(i_g - i_i) - RT\right]. \quad (A.2)$$

The so-called Clapeyron equation [15] for the vapor–solid equilibrium is approximated by Eq. (5).

$$\frac{dP_{sat}}{dT} = \frac{(i_g - i_i)}{T(v_g - v_i)} \approx \frac{P_{sat}(i_g - i_i)}{RT^2}. \quad (A.3)$$

Eq. (A.3) is rearranged for the latent heat, $(i_g - i_i)$, and x is given by Eq. (6). Therefore, Eq. (A.2) can be expressed in terms of the vapor pressure and its derivative.

$$x(u_g - u_i) = \frac{V}{mR}\frac{P_{sat}}{T}\left(\frac{RT^2}{P_{sat}}\frac{dP_{sat}}{dT} - RT\right) = \frac{V}{m}\left(T\frac{dP_{sat}}{dT} - P_{sat}\right). \quad (A.4)$$

Now the derivative of the internal energy with respect to temperatrure is written as

$$m\frac{du}{dT} = m\left\{\frac{du_i}{dT} + \frac{d[x(u_g - u_i)]}{dT}\right\} \quad (A.5)$$

for a closed system in the saturated state. From the definition of the specific heat of solid,

$$\frac{du_i}{dT} = C_i. \quad (A.6)$$

Eq. (A.3) is differentiated and simplified.

$$\frac{d\left[x(u_g - u_i)\right]}{dT} = \frac{VT}{m}\frac{d^2P_{sat}}{dT^2}. \quad (A.7)$$

Once Eqs. (A.6) and (A.7) are substituted into Eq. (A.5), the change of the internal energy with temperature for a constant volume is derived.

$$m\frac{du}{dT} = mC_i + VT\frac{d^2P_{sat}}{dT^2}. \quad (A.8)$$

References

[1] Hase T, Shibutani K, Hayashi S, Shimada R, Ogawa R, Kawate Y. Generation of 1 T, 0.5 Hz alternating magnetic field in room temperature bore of cryocooler-cooled Bi-2212 superconducting magnets. Cryogenics 1996;36:971–7.

[2] Watanabe K, Awaji S, Sakuraba J, Watazawa K, Hasebe T, Jikihara K, et al. 11 T liquid helium-free superconducting magnets. Cryogenics 1996;36:1019–25.

[3] Kobayashi T, Sato Y, Sasaki T, Mine S. Manufacturing of liquid helium free superconducting magnets for industrial use. Adv Cryog Eng 1998;43:157–63.

[4] Hasebe T, Sakuraba J, Kikihara K, Watazawa K, Mitsubori H, Sugizaki Y, et al. Cryocooler cooled superconducting magnets and their applicaitons. Adv Cryog Eng 1998;43:291297.

[5] White GK. Experimental techniques in low-temperature physics. 3rd ed. Oxford: Oxford University Press; 1979. p. 128–54.

[6] Bywaters RP, Griffin RA. A gas-gap thermal switch for cryogenic applications. Cryogenics 1973;13:344.

[7] Nast T, Bell G, Barnes C. Development of gas gap cryogenic thermal switch. Adv Cryog Eng 1981;27:1117.

[8] Chandratilleke GR, Ohtani Y, Hatakeyama H, Kuriyama T, Nakagome H. Gas-gap thermal switch for precooling of cryocooler-cooled superconducting magnets. Adv Cryog Eng 1996;41:139–46.

[9] Prenger FC, Hill DD, Daney DE, Daugherty MA, Green GF, Roth EW. Nitrogen heat pipe for cryocooler thermal shunt. Adv in Cryog Eng 1996;41:147–54.

[10] Shigi T. Some topics on recent cryogenics in Japan. International Symposium of the Korea Institute of Applied Superconductivity and Cryogenics 1998. p. 89–113.

[11] Burger JF, Holland HJ, van Egmond H, Elwenspoek M, ter Brake HJM, Rogalla H. Fast gas-gap heat switch for a microcooler. Cryocoolers 1999;10:565–74.

[12] Roth A. Vacuum technology. Amsterdam: North-Holland; 1982.

[13] Barron RF. Cryogenic systems, 2nd ed. Oxford: Oxford University Press; 1985.

[14] Friend DG. NIST thermophysical properties of pure fluids. Version 3.0. NIST Standard 12. US Department of Commerce, 1992.

[15] Sonntag RE, Borgnakke C, Van Wylen GJ. Fundamentals of thermodynamics, 5th ed. New York: Wiley; 1998.